Bull. Chem. Soc. Jpn., 71, 831—835 (1998)

Structural and Electronic Properties of Adsorbed Thiophene on Cu(111) Studied by S K-Edge X-Ray Absorption Spectroscopy

Akihito Imanishi, Toshihiko Yokoyama, Yoshinori Kitajima,† and Toshiaki Ohta*

Department of Chemistry, Graduate School of Science, The University of Tokyo, Hongo, Bunkyo-ku, Tokyo 113

†Photon Factory, Institute of Materials Structure Science, High Energy Accelerator Research Organization, Oho, Tsukuba, Ibaraki 305

(Received October 20, 1997)

The surface structure and electronic properties of 0.07 ML thiophene (C_4H_4S) adsorbed on Cu(111) have been investigated by means of S K-edge X-ray-absorption fine structure measurements. The results are comparatively discussed with the previously studied C_4H_4S/Cu(100) case. It is found that C_4H_4S molecules are adsorbed with the molecular plane parallel to the surface, as in the Cu(100) substrate. The S–Cu distance is 2.50±0.02 Å, which is significantly longer than that of Cu(100) (2.42±0.02 Å), while the S–C bond distance is 1.71±0.04 Å, somewhat shorter than the Cu(100) one (1.74±0.04 Å). Correspondingly, a smaller amount of charge transfer of (0.5±0.2) electron from the substrate to the C_4H_4S π^* orbital is estimated compared to the Cu(100) case of (1.0±0.2) electron. These findings indicate a considerably weaker interaction of thiophene with Cu(111) than with Cu(100), due to a more closely packed surface of Cu(111).

The adsorption of aromatic sulfur compounds on metal surfaces has been an important subject for understanding the mechanisms of the hydrodesulfurization process. Many investigations of thiophene C_4H_4S adsorbed on metal single crystals have been reported for Mo,[1—4] Pt,[5,6] W,[7] Cu,[8] Ni,[10—12] Rh,[13] and Pd.[14—18] In these studies, it was claimed that the adsorption structures depend on the substrate metals, temperature, and coverage. Since the reactivities on the metals were focused on in these studies, the adsorption structure or the bonding scheme has not been clarified in detail. We have investigated the adsorption structure and electronic properties of submonolayer C_4H_4S on Ni(100) and Cu(100) using S K-edge X-ray-absorption fine structure (XAFS) spectroscopy,[19] and found that on both surfaces the molecular plane is parallel to the surface, the S atom being located on the bridge site. Dissimilarities were also found between Ni(100) and Cu(100), and it was concluded that the Ni surface interacts with thiophene more strongly than Cu, because of the difference in the d-band structures between Cu and Ni.

Another interesting study is a comparison between different Miller-index surfaces of the same metal. There have been a number of papers which have clarified different adsorption properties between different Miller-index surfaces, such as CO on Pd(111) and (100),[20] CO on Cu(111) and (100),[21] and H_2 on Cu(111) and (100).[22] Very recently, we also investigated the adsorption properties of C_4H_4S on Pd(111) and Pd(100) surfaces by means of S K-edge XAFS.[23] However, no significant difference was found in the structural and electronic properties between these two surfaces beyond the experimental errors.

In the present study, we examined the surface structure and electronic properties of C_4H_4S/Cu(111) by the same XAFS technique of near-edge X-ray absorption fine structure (NEXAFS) and surface extended-X-ray-absorption fine structure (SEXAFS), while comparing them with the previous results concerning C_4H_4S/Cu(100). As revealed below, we found significant dissimilarities in the adsorption properties between Cu(111) and Cu(100). The origin of these differences is discussed in terms of the surface electronic structures of the substrates. A comparative discussion is also given concerning the previous results for Ni(100),[19] Pd(111), and Pd(100).[23]

Experimental

A commercially available Cu(111) single crystal (12 mm diameter and 3 mm thickness) was mechanically polished using 0.05 μm alumina with a mirror finish, and subsequently electrolyzed in a methanol solution of 30 vol% nitric acid at ca. 200 K with an electric current of ca. 0.1 A for 1 min. The Cu crystal was mounted in an ultrahigh vacuum (UHV) chamber (the base pressure was less than 1×10^{-8} Pa) and cleaned by means of repeated cycles of Ar^+ bombardment (500 eV at ambient temperature) and annealing up to ca. 1000 K. The cleanliness and order of the single crystal surface were verified by X-ray photoelectron spectroscopy (XPS), S K-edge NEXAFS, and low energy electron diffraction (LEED). From the fluorescence yield at the S K-edge, the amount of residual S atoms was estimated to be less than 0.003 ML, where one ML (monolayer) is defined as the number of Cu atoms in the first layer of the Cu(111) surface.

The clean crystal was subsequently dosed with ca. 5 L C_4H_4S (1 L = 1×10^{-6} Torr·s; 1 Torr = 133.322 Pa) at ca. 220±10 K, which was purified by means of a few cycles of freezing with liquid N_2 under a high vacuum and melting at ambient temperature. The temperature was monitored with a chromel–alumel thermocouple spot-welded on a Ta sheet, which was inserted between the edge of the sample and a Cu wire wound round the sample. In order to avoid any electron-induced molecular dissociation, neither AES (Auger Electron Spectroscopy) nor LEED measurements were performed after C_4H_4S exposure to Cu(111).

S K-edge NEXAFS (2460—2510 eV) and SEXAFS (2400—3000 eV) measurements were carried out at the soft X-ray double-crystal monochromator station BL-11B[24,25] of the Photon Factory (positron ring energy of 2.5 GeV and stored ring current of 350—250 mA) in the Institute of Materials Structure Science, High Energy Accelerator Research Organization (KEK-PF). The factor of linear polarization was estimated to be larger than 0.97 for monochromatized photons, and the energy resolution around the S K-edge region was ca. 1 eV. The absolute photon energy was calibrated with the strong resonance of K_2SO_4 ($S1s \rightarrow t_2$) appearing at 2481.7 eV. The S-K fluorescence yield detection was employed using a UHV-compatible gas-flow proportional counter with P10 gas (10% CH_4 in Ar).[26] The electric current from a Cu mesh upstream of the sample crystal was monitored simultaneously and used as the intensity of the incident X-rays (I_0) in order to normalize the fluorescence yield spectra (I). During the spectroscopic measurements, the sample temperature was kept constant at 92 ± 2 K. The X-ray incident angle (θ) was set at 90° (normal X-ray incidence) and 15°. The 55° spectrum was also taken for NEXAFS.

S K-edge NEXAFS

Figure 1 shows angular dependent S K-edge NEXAFS spectra of submonolayer C_4H_4S on Cu(111), together with those of a randomly oriented multilayer of C_4H_4S and submonolayer C_4H_4S on Ni(100) and Cu(100), reported previously.[19] The S coverage of a submonolayer of C_4H_4S on Cu(111) was estimated from the S K-edge jump (normalized S-K fluorescence intensity). Using the $(\sqrt{17}\times\sqrt{17})R14°$ atomic S/Cu(100) system as a reference (0.47 ML), the coverage was found to be 0.07 ML, which is comparable with the Cu(100) case.[19] With the assumption of a completely flat orientation of C_4H_4S molecules, a possible one-layer saturation coverage is estimated to be ca. 0.11 ML for Cu(111) using the van der Waals molecular size. This implies that the present system should be in a submonolayer state containing a smaller amount of S than that of the hypothetical saturated one layer.

Although one intense broad resonance appears at 2473.3 eV in the spectrum of multilayer C_4H_4S, this peak is known to consist of two resonances: one is the S1s-to-π^* transition at 2473.0 eV, the other is S1s-to-σ^*(S–C) at 2473.5 eV.[27] A noticeable polarization dependence can be seen in the submonolayer spectra in Fig. 1. The first intense resonance clearly exhibits energy shifts between the 90° and 15° spectra. We can assign two peaks at 2472.3 eV (appearing in the 15° spectrum) and 2473.5 eV (in the 90° spectrum) to π^* and σ^*(S–C) transitions, respectively. The σ^*(S–C) resonance of the submonolayer spectrum is most enhanced at a normal X-ray incidence and is almost diminished at grazing incidence. On the other hand, the π^* resonance is most enhanced at grazing incidence. This implies a flat-lying orientation of the molecular plane on Cu(111), as in the cases of Cu(100) and Ni(100).[19]

Since the spectra are normalized by their edge-jump in Fig. 1, we can compare the peak intensities directly with each other, and find that the intensity of the π^* resonance at $\theta = 15°$ in the submonolayer spectra becomes suppressed in the sequence Cu(111), Cu(100), and Ni(100). The suppression of the π^* resonance intensity might be caused by charge transfer from the substrates to the π^* orbital, because the molecular orientation on these surfaces should essentially be the same. For a quantitative comparison, however, the 55° spectra should be used since the polarization dependence is effectively canceled at the magic angle of 55°. A spectral analysis[28] for the 55° spectra was carried out (shown in Fig. 2). As a result, the normalized π^* intensity for Cu(111) was found to be reduced to 75 ± 9% of the multilayer value, implying that 25 ± 9% of the π^* orbital was occupied, and 0.5 ± 0.2 electron was thus transferred from the Cu(111) substrate to the C_4H_4S π^* orbital. The amount of charge transfer is significantly smaller than those of Cu(100) (1.0 ± 0.2 electron) and Ni(100) (1.4 ± 0.2 electrons).[19]

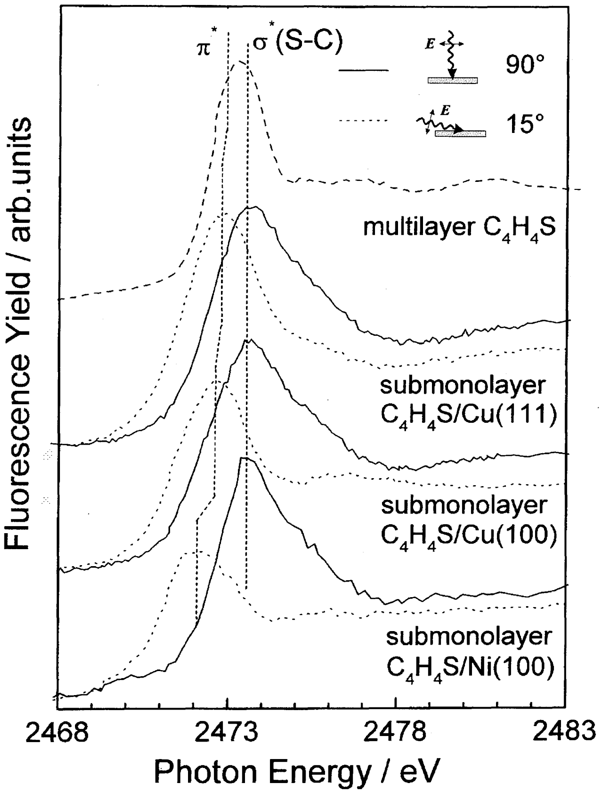

Fig. 1. S K-edge NEXAFS spectra of multilayer C_4H_4S[19] at the X-ray incidence angle of 55° (dashed line) and submonolayer C_4H_4S on Cu(111), Cu(100),[19] and Ni(100)[19] at 90° (dotted lines) and 15° (solid lines).

S K-edge SEXAFS

Extraction of the EXAFS function $\chi(k)$ (k is the photoelectron wave number) was carried out according to the well-established procedures: pre- and post-edge background subtraction and subsequent normalization with atomic absorption coefficients.[29,30] A few glitches were artificially eliminated prior to the analysis. Figure 3 shows the extracted $\chi(k)$ functions of submonolayer C_4H_4S/Cu(111), and

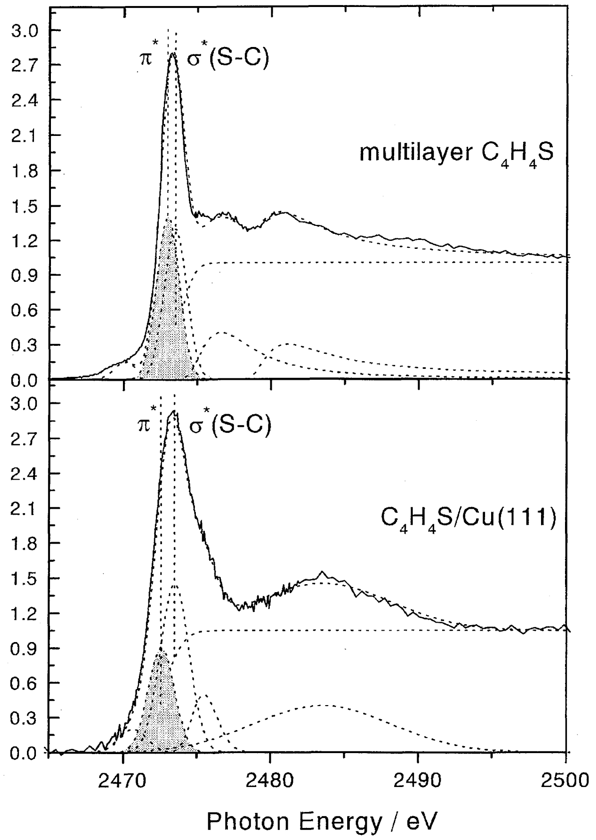

Fig. 2. The spectral analysis of S K-edge NEXAFS from the multilayer and C_4H_4S on Cu(111) at 55° incident angle. Energy positions of the π^* and σ^* resonance peaks of submonolayer C_4H_4S/Cu(111) are derived from the grazing and normal incidence spectra in Fig. 1.

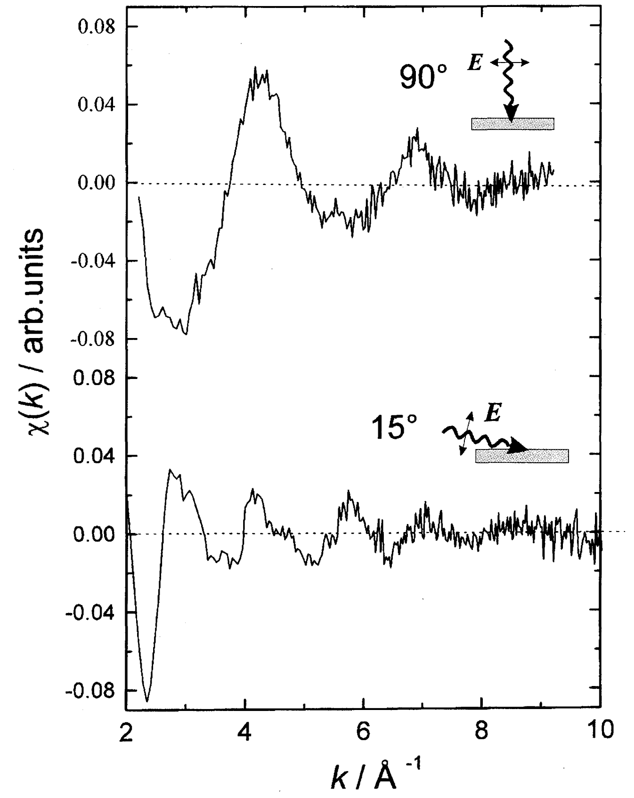

Fig. 3. S K-edge SEXAFS oscillation function $\chi(k)$ of submonolayer C_4H_4S on Cu(111) at 90° and 15°.

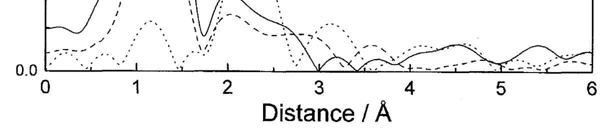

Fig. 4. Fourier transforms of the S K-edge SEXAFS oscillation functions $k^2\chi(k)$ of multilayer C_4H_4S[19] (dashed line) and submonolayer C_4H_4S on Cu(111) at 90° (dotted line) and 15° (solid line). Note that each peak is slightly shifted from the real bond distance by the phase shift.

the corresponding Fourier transforms ($\Delta k = 2.3 - 10.2$ Å^{-1}) are shown in Fig. 4, in which the Fourier transform of the multilayer is also given. The peak appearing at ca. 1.2 Å can be ascribed to intramolecular S–C coordination. It shows a strong polarization dependence, and is enhanced at normal X-ray incidence. This indicates that the S–C bond is lying flat on the surface, being consistent with the above NEXAFS results. The peak at ca. 2.1 Å in the 15° Fourier transform is ascribed to the S–Cu shell, while in the 90° one the second neighbor S–C shell should also appear, judging from the Fourier transform of a multilayer.

A curve-fitting analysis in k space was performed after Fourier filtering of the contribution of interest ($\Delta R =$ 0.75—2.70 Å). For the S–C shell, the multilayer C_4H_4S spectrum was used as a standard (the S–C distance of 1.71 Å). For the S–Cu shell, a theoretically evaluated $\chi(k)$, given by FEFF6,[31,32] was employed. The fitting variables were $N^*S_0^2$ (effective coordination number (N^*) multiplied by the intrinsic loss factor (S_0^2)), the interatomic distance (R), the edge energy shift (ΔE_0), and the EXAFS Debye–Waller factor (σ^2). The S–Cu distance ($R_{\text{S–Cu}}$) was found to be 2.50±0.02 Å, which is considerably longer than the Cu(100) one of 2.42±0.02 Å.[19] We could not determine the S adsorption site from the polarization dependence of the effective coordination number (N^*) of the S–Cu shell, because the Fourier transform of the 90° spectrum in Fig. 4 shows a significant superposition of the second neighbor S–C shell. On the other hand, the nearest neighbor S–C distance ($R_{\text{S–C}}$) was found to be 1.71±0.05 Å, which is somewhat shorter than the Cu(100) one of 1.74±0.05 Å, though these lie within the estimated experimental errors. The value of 1.74±0.05 Å for Cu(100), which was obtained by a re-analysis of the previous SEXAFS spectra from C_4H_4S/Cu(100), is slightly different from the previously reported one (1.71±0.05 Å). The reason

Table 1. Structural and Electronic Data of Multilayer C_4H_4S and Submonolayer C_4H_4S on Cu(111), Cu(100), Ni(100), Pd(111), and Pd(100) Obtained by the Surface XAFS Experiments

System	Charge transfer/e	S–C distance/Å	S-metal distance/Å	π* resonance energy/eV	Ref.
Multilayer	0.0	1.71		2473.0	19)
Cu(111)	0.5±0.2	1.71±0.05	2.50±0.02	2472.6	This work
Cu(100)	1.0±0.2	1.74±0.05	2.42±0.02	2472.3	19)
Pd(111)	1.1±0.2	1.73±0.05	2.31±0.03 2.94±0.05	2472.3	23)
Pd(100)	1.2±0.2	1.73±0.05	2.30±0.03 2.95±0.05	2472.3	23)
Ni(100)	1.4±0.2	1.80±0.05	2.20±0.02	2471.9	19)

On Cu(100) and Ni(100), S sits on the bridge site, while on Pd(100) and (111) S locates between the atop and bridge sites. Thus, two inequivalent S–Pd distances are given for the Pd substrates.

for such an uncertainty of the bond distance comes from the ambiguity in the post-edge background subtraction. This is a substantial problem of EXAFS, to which the contribution by a low-Z atom, such as C and O, is very small.

Discussion

Table 1 summarizes the obtained structural and electronic parameters of C_4H_4S/Cu(111), together with those of multilayer C_4H_4S/Cu(100),19) C_4H_4S/Pd(111),23) C_4H_4S/Pd(100),23) and C_4H_4S/Ni(100).19) The amount of charge transfer from the substrate to the antibonding π^* orbital on Cu(111) is considerably smaller than that on Cu(100). The S–C bond is elongated by 0.03 Å on Cu(100) compared to the multilayer one, while on Cu(111) no meaningful elongation was detected. Although the difference in the S–C bond length is within the errors, these findings are consistent with each other. Including all of the substrates given in Table 1, the interaction between the substrate and C_4H_4S is strengthened in the sequence Cu(111) < Cu(100) ≈ Pd(111) ≈ Pd(100) < Ni(100). It is easily understood that Ni shows the strongest interaction because of its higher reactivity than Cu and Pd.

In the S K-edge NEXAFS spectra, the lower energy shift of the π^* resonance was observed in the order of the interaction strength. The energy shift clearly coincides with the trend of the charge transfer and the S–C bond length. Although the energy shift of the π^* resonance cannot be explained, because of the complicated origins of NEXAFS, there should be a certain physical meaning for this relationship. Some sophisticated theoretical consideration is required to solve the question.

The differences in the adsorption properties between Cu(111) and Cu(100) could be explained based on the dissimilarity of the surface atomic densities. The Cu(111) surface consists of a more closely packed Cu atoms than Cu(100), thus leading to a broader density of states (DOS) near to the Fermi level.22) Because of a more dilute DOS in Cu(111), the Cu(111) surface should be less active and the amount of charge transfer from the substrate to C_4H_4S is smaller.

On the contrary, no difference was observed for Pd(111) and Pd(100),23) as shown in Table 1. The different trend between Pd and Cu could be explained by the different interaction mechanisms. In the C_4H_4S/Pd case, the Pd 4d orbitals interact with C_4H_4S, while for Cu the 4sp band should play an important role for the bonding, because the Cu 3d bands locate in a deep energy range. Since the d band is more localized than the sp band, the atomic character might dominate the band nature in Pd, leading to less change between the (111) and (100) surfaces. On the other hand, in the Cu case, the sp band is fully delocalized and is easily influenced by the change of the Miller index.

Conclusions

The surface structures and electronic properties of submonolayer C_4H_4S adsorbed on Cu(111) were investigated by means of S-K edge SEXAFS and NEXAFS. C_4H_4S adsorbs molecularly with the molecular plane parallel to the surfaces, accompanied by charge transfer (0.5±0.2 electron) from the substrate to the π^* orbital. The intramolecular S–C bond length was determined to be 1.71±0.05 Å, and the S–Cu distance was 2.50±0.02 Å. These results were compared to the previous results of Cu(100), Ni(111), Pd(111), and Pd(100). Significant differences in the adsorption behaviors were found amongst these substrates and were discussed in terms of the different electronic structures of the substrates.

The authors are grateful for the financial support of Grant-in-Aids for Scientific Research Nos. 05403010 and 07454060. This work was performed under the approval of Photon Factory Program Advisory Committee (PF-PAC No. 94G030).

References

1) J. T. Roberts and C. M. Friend, *Surf. Sci.*, **186**, 201 (1987).

2) A. J. Gellman, M. H. Farias, M. Salmeron, and G. A. Somorjai, *Surf. Sci.*, **136**, 217 (1984).

3) F. Zaera, E. B. Kollin, and J. L. Gland, *Surf. Sci.*, **184**, 75 (1987).

4) D. G. Kelly, M. Salmeron, and G. A. Somorjai, *Surf. Sci.*, **175**, 465 (1986).

5) J. Stöhr, J. L. Gland, E. B. Kollin, R. J. Koestner, A. L. Johnson, E. L. Muetterties, and F. Sette, *Phys. Rev. Lett.*, **53**, 2161 (1984).

6) J. F. Lang and R. I. Masel, *Surf. Sci.*, **183**, 44 (1987).

7) R. E. Preston and J. B. Benziger, *J. Phys. Chem.*, **89**, 5010 (1985).

8) N. V. Richardson and J. C. Campuzano, *Vacuum*, **31**, 449 (1981).

9) B. A. Sexton, *Surf. Sci.*, **163**, 99 (1985).

10) G. R. Schoofs, R. E. Preston, and J. B. Benziger, *Langmuir*, **1**, 313 (1985).

11) J. Stöhr, E. B. Kollin, D. A. Fischer, J. B. Hastings, F. Zaera, and F. Sette, *Phys. Rev. Lett.*, **55**, 1468 (1985).

12) S. Yagi, Docter Thesis, Hiroshima University, 1995.

13) F. P. Netzer, E. Bertel, and A. Goldmann, *Surf. Sci.*, **201**, 257 (1988).

14) I. M. Abdelrehim, N. A. Thornburg, J. T. Sloan, and D. P. Land, *Surf. Sci.*, **298**, L169 (1993).

15) T. E. Caldwell, I. M. Abdelrehim, and D. P. Land, *Surf. Sci.*, **367**, L26 (1996).

16) A. J. Gellman, *Langmuir*, **7**, 827 (1991).

17) A. J. Gellman, *J. Am. Chem. Soc.*, **113**, 4435 (1991).

18) A. J. Gellman, *J. Phys. Chem.*, **96**, 790 (1992).

19) A. Imanishi, S. Yagi, T. Yokoyama, Y. Kitajima, and T. Ohta, *J. Electron Spectrosc. Relat. Phenom.*, **80**, 151 (1996).

20) K. Yoshioka, F. Kitamura, M. Takeda, M. Takahashi, and M. Ito, *Surf. Sci.*, **227**, 90 (1990).

21) C. J. Hirschmugl and G. P. Williams, *Phys. Rev. B*, **B52**, 14177 (1995).

22) P. Kratzer, B. Hammer, and J. K. Norskov, *Surf. Sci.*, **359**, 45 (1996).

23) S. Terada, T. Yokoyama, M. Sakano, A. Imanishi, Y. Kitajima, M. Kiguchi, Y. Okamoto, and T. Ohta, to be published.

24) T. Ohta, P. M. Stefan, M. Nomura, and H. Sekiyama, *Nucl. Instrum. Methods A*, **A246**, 373 (1986).

25) Y. Kitajima, *J. Electron Spectrosc. Relat. Phenom.*, **80**, 405 (1996).

26) M. Funabashi, T. Ohta, T. Yokoyama, Y. Kitajima, and H. Kuroda, *Rev. Sci. Instrum.*, **60**, 2505 (1989).

27) Y. Takata, Y. Kitajima, H. Aga, S. Yagi, T. Asahi, T. Yokoyama, K. Tanaka, and T. Ohta, *Jpn. J. Appl. Phys.*, **32**, Suppl. 2, 350 (1993).

28) J. Stöhr, "NEXAFS Spectroscopy," Springer, Berlin (1992).

29) "X-Ray Absorption: Principles, Applications, Techniques of EXAFS, SEXAFS, and XANES," ed by D. C. Koningsberger and R. Prins, John Wiley & Sons, New York (1988).

30) T. Yokoyama, H. Hmamatsu, and T. Ohta, "EXAFS Analysis Program EXAFSH Version 2.1," The University of Tokyo (1994).

31) J. J. Rehr, J. Mustre de Leon, S. I. Zabinsky, and R. C. Alberts, *J. Am. Chem. Soc.*, **113**, 5135 (1991).

32) S. I. Zabinsky, J. J. Rehr, A. Ankdinov, R. C. Albers, and M. J. Eller, *Phys. Rev. B*, **B52**, 2995 (1995).